AD-A078 231 SCIENCE APPLICATIONS INC MCLEAN VA F/G 20/9
STRONGLY TURBULENT STABLIZATION OF ELECTRON BEAM-PLASMA INTERAC--ETC(U)
NOV 79 H P FREUND , I HABER , P PALMADESSO NASA-W-14365
UNCLASSIFIED NRL-MR-4127 NL

| OF |
ADA
078231

END
DATE
FILMED
1 -80
DDC

LEVEL II

NRL Memorandum Report 4127

Strongly Turbulent Stabilization of Electron Beam–Plasma Interactions

H. P. FREUND

Science Applications, Inc.
McLean, Virginia 22101

AND

I. HABER, P. PALMADESSO AND K. PAPADOPOULOS

Plasma Physics Division

November 9, 1979

NAVAL RESEARCH LABORATORY
Washington, D.C.

SECURITY CLASSIFICATION OF THIS PAGE (When Data Entered)

REPORT DOCUMENTATION PAGE

READ INSTRUCTIONS BEFORE COMPLETING FORM

1. REPORT NUMBER: NRL Memorandum Report 4127
2. GOVT ACCESSION NO.:
3. RECIPIENT'S CATALOG NUMBER:

4. TITLE (and Subtitle): STRONGLY TURBULENT STABILIZATION OF ELECTRON BEAM–PLASMA INTERACTIONS

5. TYPE OF REPORT & PERIOD COVERED: Interim report on a continuing NRL problem.

6. PERFORMING ORG. REPORT NUMBER:

7. AUTHOR(s): H. P. Freund*, I. Haber, P. Palmadesso and K. Papadopoulos

8. CONTRACT OR GRANT NUMBER(s):

9. PERFORMING ORGANIZATION NAME AND ADDRESS: Naval Research Laboratory, Washington, DC 20375

10. PROGRAM ELEMENT, PROJECT, TASK AREA & WORK UNIT NUMBERS: NRL Problem 67A03-16B; ONR & NASA Cont. W-14365

11. CONTROLLING OFFICE NAME AND ADDRESS: Office of Naval Research, Arlington, VA 22217 and National Aeronautics and Space Administration, Washington, DC 20546

12. REPORT DATE: November 9, 1979

13. NUMBER OF PAGES: 42

14. MONITORING AGENCY NAME & ADDRESS (if different from Controlling Office):

15. SECURITY CLASS. (of this report): UNCLASSIFIED

15a. DECLASSIFICATION/DOWNGRADING SCHEDULE:

16. DISTRIBUTION STATEMENT (of this Report)

Approved for public release; distribution unlimited.

17. DISTRIBUTION STATEMENT (of the abstract entered in Block 20, if different from Report)

18. SUPPLEMENTARY NOTES

*Science Applications, Inc., McLean, Virginia 22101

This research was sponsored partially by the Office of Naval Research and by the National Aeronautics and Space Administration under Contract W-14365.

19. KEY WORDS (Continue on reverse side if necessary and identify by block number)

Strong turbulence
Langmuir turbulence
Electron beam-plasma stabilization
Langmuir solitons
Oscillating two stream instability

20. ABSTRACT (Continue on reverse side if necessary and identify by block number)

The stabilization of electron beam interactions due to strongly turbulent nonlinearities is studied analytically and numerically for a wide range of plasma parameters. A fluid mode coupling code is described in which the effects of electron and ion Landau damping and linear growth due to the energetic electron beam are included in a phenomenological manner. Stabilization of the instability is found to occur when the amplitudes of the unstable modes exceed the threshold of the oscillating two stream instability. The coordinate space structure of the turbulent spectrum which results

(Continues)

DD FORM 1 JAN 73 1473 EDITION OF 1 NOV 65 IS OBSOLETE
S/N 0102-014-6601

SECURITY CLASSIFICATION OF THIS PAGE (When Data Entered)

4 08 404

20. Abstract (Continued)

clearly shows that soliton-like structures are formed by this process. Phenomenological models of both the initial stabilization and the asymptotic states are developed. Scaling laws between the beam-plasma growth rate and the fluctuations in the fields and plasma density are found in both cases, and shown to be in good agreement with the results of the simulation.

CONTENTS

I. INTRODUCTION 1

II. THE NUMERICAL SIMULATION 3

III. THEORETICAL CONSIDERATIONS 8

A. The Linearized Dispersion Equation. 8

B. The Phenomenological Description. 14

IV. SUMMARY AND DISCUSSION 20

ACKNOWLEDGMENT 24

APPENDIX - The Linearized OTS Dispersion Equation 25

REFERENCES 28

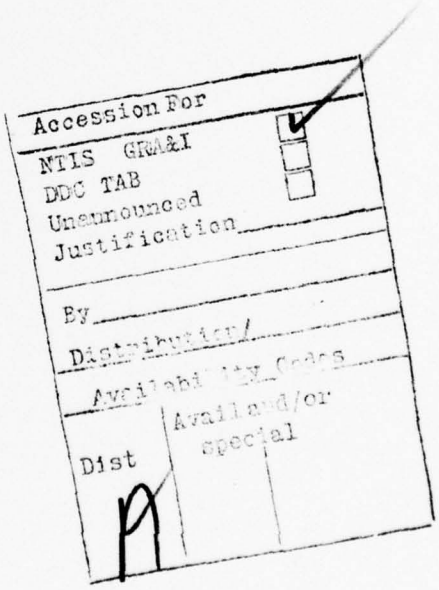

STRONGLY TURBULENT STABILIZATION OF ELECTRON BEAM—PLASMA INTERACTIONS

I. Introduction

The interaction of relativistic and non-relativistic electron beams with a plasma remains an important topic of research. In addition to the usual applications both to space plasmas and the heating of linear devices in the laboratory, a resurgence of interest in this problem has occurred due to possible applications in toroidal magnetic confinement devices. For example, Mohri et al.[1] have injected relativistic electron beams into toroidal devices, and Papadopoulos et al.[2] have proposed the in situ formation of relativistic electron beams in tokamaks as a current driver, for long pulse operation, and for supplementary heating. Finally, it should be mentioned that several of the spheromak concepts require relativistic electron beam drivers. Any assessment of these concepts requires a good theoretical basis of prediction of the beam relaxation process. It is our purpose in this work to provide such an understanding based upon computational means.

The failures of the quasilinear (or any weak turbulence theory) to describe the beam relaxation process is well-known in the literature[3-6], and the strong turbulence theory has been successful in resolving many of the discrepancies between theory and experiment.[3-8] However, in view of the complexity of the problem, several ad hoc simplifications are commonly made in the name of analytic tractability. We present, here, the results of a numerical solution of the strong turbulence equations which describe the temporal evolution of a beam streaming through a plasma. The model we employ is one-dimensional, which is easily justified in the presence of even a modest magnetic field. We neglect the self-consistent interaction of the waves with the beam

Note: Manuscript submitted October 9, 1979.

particles by the assumption of a constant linear growth rate for the beam-plasma instability. This assumption can be justified a posteriori, and will be discussed in more detail in the concluding section. Following the presentation of the simulation results, we develop a phenomenological model to describe the beam relaxation-process in an attempt to reproduce the scalings of the fluctuation quantities with the linear growth rate.

In addition, Manheimer and Papadopoulos[9] have demonstrated that the equations which govern the nonlinear coupling between Langmuir and ion acoustic waves are formally equivalent to Zakharov's equations[10] for Langmuir solitons. As a consequence, it is reasonable to expect the formation of soliton-like structures to occur by means of this mechanism, and such a result is, in fact, clearly shown by the numerical solution of the dynamical equations.

The organization of the paper is as follows. In Sec. II, we discuss the numerical simulation. The basic equations are given and the simulation code is briefly described prior to a description of the results. Extensive results are presented which describe the scaling of the fluctuation levels at the initial stabilization and in the asymptotic, quasi-steady state, regime with linear growth rate. In Sec. III, we describe the pertinent theoretical considerations including a brief discussion of the linearized growth rate of the nonlinear interaction, and a presentation of the phenomenological model which describes the scaling laws. A summary and discussion appears in Sec. IV.

II. The Numerical Simulation

The basic equations to be solved are well known

$$\left[i\frac{\partial}{\partial t} - \frac{3}{2}\omega_e(k\lambda_e)^2\right] E(k) = i(\gamma_k - \nu_{ek})E(k) + \frac{\omega_e}{2n_o}\int dk'\,\delta n(k-k')E(k'), \tag{1}$$

$$\left[\frac{\partial^2}{\partial t^2} + \nu_{ik}\frac{\partial}{\partial t} + k^2c_s^2\right] \delta n(k) = -\frac{k^2}{16\pi M}\int dk'E(k-k')E^*(-k'), \tag{2}$$

where $E(k)$ and $\delta n(k)$ are the mode amplitudes of the electron and ion oscillations, γ_k is the growth rate of mode k of the beam-driven electron plasma oscillations, ν_{ek} and ν_{ik} are the total damping rates (collisional and collisionless) due to electrons and ions, $\omega_e^2 \equiv 4\pi e^2 n_o/m$, m and M are the electron and ion masses, and c_s is the ion acoustic speed. In the derivation of (1) and (2), we followed Zakharov's procedure and (1) averaged over the fast time scale ω_e^{-1}, (2) neglected the electron nonlinearity, and (3) described the motion of the electrons and ions on the basis of the hydrodynamic equations with phenomenological damping (i.e., ν_{ek} and ν_{ik}). These equations emphasize the importance of the coupling between the electron and ion modes. Note that Eqs. (1) and (2) are the k-space representations of the equations used in the study of plasma solitons.

In the usual quasilinear theory, the second term on the right-hand-side of Eq. (1) is absent, since only electron modes are considered. As

a result, stabilization is achieved only when $\gamma_k = 0$ and a plateau in velocity space is formed. However, consideration of the effect of the ponderomotive force due to the electron plasma oscillations (i.e., the right-hand-side of Eq. (2))on the ions permits the self-consistent excitation of ion acoustic oscillations. Thus, stabilization can be achieved, for $\gamma_k > 0$, when the level of ion oscillations reaches a level at which the right-hand-side of (1) vanishes or becomes negative. It should be noted that in models in which the ions are treated as a motionless, neutralizing background, the right-hand-side of (2) vanishes due to the M^{-1} dependence and this effect disappears.

Eqs. (1) and (2) describe the time evolution of the spatial Fourier spectrum of the electric field and ion density fluctuations. Under the assumption of periodic boundary conditions, the spectrum goes from a continuous to a discrete one and the nonlinear coupling terms become sums rather than integrals. Further, because of the increase in damping with decreasing wavelength, the short wavelength terms can be neglected and a truncation of the infinite sum over modes is possible. The system of ordinary differential equations which results has been integrated numerically using a deferred limit integrator routine with an adjustable convergence parameter. Numerical tests were performed to insure the insensitivity of the physical results to variations in the numerical parameters. In general, a mode spectrum $-.34 \leq k\lambda_e \leq .34$ was found to be adequate, with a separation of $\Delta(k\lambda_e) = .02$ between the modes. The electron damping decrement was assumed to be of the form $\nu_{ek} \sim k^{-3} \exp(-1/2\ k^2\lambda_e^2)$ for $|k\lambda_e| > .16$ and zero otherwise; and a non-zero growth rate (γ_k) was assumed only for a single mode, which, unless otherwise stated will correspond to $k_o\lambda_e = .02$,

and will be denoted by γ_o. The ion damping decrement was taken to vary linearly in k; and we use $\nu_{ik} \sim (m/M)\, k\lambda_e$.

Results of the simulation which show the typical time evolution of the beam plasma system are shown in Fig. 1, in which we plot (1) the total spectral energy density of the plasma modes (denoted by W_{tot}), (2) the spectral energy density of the beam mode (denoted by W_o), and (3) the root-mean-square fluctuation of the ion density for the case in which $\gamma_o/\omega_e = 3 \times 10^{-4}$. As seen in the figure, the first stage of the interaction is linear growth during which the amplitude of W_o (and, hence, W_{tot}) increases rapidly while the ion density fluctuations remain at a relatively low level. The turbulent phase sets in abruptly when W_o exceeds the nonlinear threshold. During this sudden onset phase, the level of ion density fluctuations increases rapidly, and wave energy is transferred from the beam-resonant mode at a rate faster than the linear growth rate. Stabilization is achieved when the nonlinear energy transfer rate is faster than the linear growth rate. On a longer time scale, an asymptotic state is established with slowly varying levels of spectral energy density and ion density fluctuations. The turbulent nature of the quasi-steady state, however, is indicated by the rapid fluctuations in W_o (shown schematically in the figure) which are indicative of a strong coupling between the modes of the system.

In order to determine the scaling of the spectral energy density in the Langmuir oscillations and the ion density fluctuations with the linear growth rate in both the sudden onset and asymptotic phases, we have run a series of simulations with $\gamma_o/\omega_e = .0001 - .0010$. The results are displayed in Figs. 2-6.

Fig. 2 shows the amplitude of the first peak in $W_o(\simeq W_{tot})$ as a function of γ_o/ω_e during the sudden onset phase, for three choices of $k_o\lambda_e$ (=0.02, 0.06, and 0.10), in which it is evident that two regimes exist. It should be noted here that while changes in $k_o\lambda_e$ (which corresponds to changes in v_e/v_b) have an effect upon the saturation level of W_o, there is little change in the overall scaling properties. We find that for low growth rates, the peak pump-energy scales as $(W_o)_{max} \sim \gamma_o$, while for higher growth rates $(W_o)_{max} \sim \gamma_o$. The transition occurs for $\gamma_o/\omega_e \simeq .0003$. The corresponding peaks in the ion density fluctuations are found to scale as $(\delta n/n_o)_{rms} \sim \gamma_o$ over the range, and is shown in Fig. 3 for $k_o\lambda_e = 0.02$. The effect of variations in $k_o\lambda_e$ will be treated in more detail later in this work; however, in the meantime we consider the case of $k_o\lambda_e = .02$ in more detail.

Fig. 4 shows the level of ion density fluctuations averaged over time during the asymptotic regime (i.e., the long time scale result after stabilization is achieved) versus γ_o, and we find that a result of $\langle(\delta n/n_o)_{rms}\rangle_\infty \sim \gamma_o$ is indicated. The corresponding result for W_{tot} in the asymptotic regime is given in Fig. 5, for which we also obtain that $\langle W_{tot}/n_o T_e\rangle_\infty \sim \gamma_o$. Finally, we plot the averaged energy deposition rate (i.e., the rate at which energy is extracted from the beam) versus γ_o in Fig. 6, and a roughly linear relationship is found here as well.

In order to study the time variation of the field and density fluctuations in coordinate space, the spatial Fourier transforms are inverted at selected time intervals. The essential characteristics of the coordinate dependence of the solution are shown in Figs. 7a-7d in which

we plot the ion density fluctuations and the magnitude of the electric field fluctuations as a function of position for the case which corresponds to that shown in Fig. 1. The normalization chosen is to the maximum values attained by the ion density fluctuation and the electric field fluctuation respectively. Fig. 7a depicts the state of the field and density fluctuations late in the linear phase of the interactions, and just prior to the onset of the strongly nonlinear regime. The situation shown in Fig. 7b corresponds to a slightly later time just prior to that shown in Fig. 1 when the total spectral energy density reaches a maximum. As noted earlier, the processes of soliton formation and parametric stabilization are linked, and it is evident that this figure describes the early phases of both processes. Fig. 7c corresponds to the point at which the soliton reaches maximum amplitude. It should be pointed out that the solitons reach peak amplitude very quickly once the nonlinear effects become important, and that Fig. 7c describes the system prior to the attainment of a steady state. In this phase of the interaction the total spectral energy density is decreasing. Finally, Fig. 7d describes the system shortly after the steady state has been achieved. The total spectral energy density and soliton amplitude vary little beyond this point.

In order to investigate the effect of varying choices of $k_o\lambda_e$ in more detail, we plot the initial peak in W_o versus k_o for several choices of γ_o in Fig. 8. It is clear that while the scaling between $(W_o)_{max}$ and k_o varies with γ_o, we typically find that $(W_o/n_oT_e)_{max} \simeq (k_o\lambda_e)^{-.83}$.

III. Theoretical Considerations

A phenomenological model of the onset phase of the interaction was produced in ref. 3 by stressing the analogy in the linear regime between the formation of cavities by a modulationally unstable wave spectrum in the strong turbulence regime and the well-known theory of parametric instabilities. Once the threshold is reached (i.e., $W_o/n_o T_e \geq k^2\lambda_e^2$) the wave spectrum becomes unstable and forms cavities out of the uniform Langmuir turbulence. This involves the transfer of energy to shorter wavelength modes, which permits interaction with the background plasma.

The principal purpose of this section is to construct a phenomenological model of the nonlinear beam-plasma interaction which predicts the scaling laws between (1) the fluctuation quantities at the time of initial stabilization, (2)the average values of the fluctuations during the asymptotic phase with the linear growth rate. This requires a knowledge of the nonlinear growth rate and, as a result, this section is divided into two parts. In the first, we consider the parametric growth rate in an effort to develop some insight into the scaling of the nonlinear growth rate on the wavelength and wavelength spread of the unstable spectrum as well as on the effect of electron and ion damping. Using the estimates and scaling found in the first part, we develop the phenomenological model of the nonlinear stages of the interaction in the second part of the section.

A. The Linearized Dispersion Equation

Useful insights into the nature of the nonlinear stabilization mechanism can be obtained by consideration of the beam generated waves

as a pump spectrum with frequencies in the vicinity of the plasma frequency and with wavelengths in the range $k_o - \Delta k_o/2 < k < k_o + \Delta k_o/2$. We then examine the linear stability of the spectrum using Eqs. (1) and (2). This is analogous to determination of the growth rates of the parametric instabilities excited by the beam modes, and stabilization of the beam-plasma instability can be expected when the nonlinear term on the right-hand-side of (1) dominates over the term in γ_k (i.e., the linear growth rate).

The linear dispersion equation takes the form

$$\omega(\omega + i\nu_{ik}) - k^2 c_s^2 = -\frac{3}{4}\frac{m}{M}(k\lambda_e)^4 \omega_e^2 \int_{-\infty}^{\infty} dk' \frac{W_o(k')}{n_o T_e} \times \frac{\omega_e^2}{\frac{9}{4}\omega_e^2 (k\lambda_e)^4 - \left[(\omega + i\nu_{ek} - i\gamma_k) - 3\omega_e (k\lambda_e)(k'\lambda_e)\right]^2} , \qquad (3)$$

where $W_o(k') = |E(k')|^2/8\pi$ is the wave energy density in the beam-driven modes. For a given spectrum $W_o(k')$, one can find the parametric growth rate as well as the regimes of importance in the spectral transfer of energy. In this section, we describe the spectrum of beam-driven modes by means of a Lorentzian distribution of the form

$$W_o(k') \approx \frac{W_o}{\pi} \frac{\Delta k_o}{(k' - k_o)^2 + \Delta k_o^2} . \qquad (4)$$

It is clear that $\lim_{\Delta k_o \to 0} W_o(k') = W_o\, \delta(k'-k_o)$; therefore, such a model spectrum is useful in the determination of the effects of a pump spectrum with both finite wavelength and finite bandwidth on the dispersion equation. A detailed discussion of the dispersion equation is beyond the scope of this work, and we shall present only a brief discussion of the solutions to (3) and (4) in the text. The interested reader is referred to the Appendix for further detail.

In the limit in which $k_o \ll k$, the threshold condition for the oscillating two stream instability can be written in the form

$$\frac{W_o}{n_e T_e} > 3(k\lambda_e)^2 \left(1 - 4\,\frac{k_o^2}{k^2}\right), \tag{5}$$

and it is clear that the effect of finite k_o is to reduce the threshold required for instability. It can also be shown that $(\omega = \omega_o + i\gamma)$

$$\omega_o \cong \frac{9}{4}\,\omega_e\,\frac{k_o}{k}\,\frac{m}{M}\,\frac{W_o}{n_o T_e}\,(k\lambda_e)^4 \left[\frac{9}{4}\,(k\lambda_e)^4 + \frac{\gamma^2}{\omega_e^2}\right]^{-2} \tag{6}$$

and

$$\gamma^2 \cong \frac{3}{4}\,\omega_e^2\,\frac{m}{M}\,(k\lambda_e)^2 \left[\frac{W_o}{n_o T_e} - 3(k\lambda_e)^2 \left(1 - 4\,\frac{k_o^2}{k^2}\right)\right]$$

$$\times \left[\frac{m}{M} + \frac{9}{4}\,(k\lambda_e)^2 \left(1 - 4\,\frac{k_o^2}{k^2}\right)\right]^{-1}, \tag{7}$$

subject to the requirement that

$$\tfrac{3}{4}(k\lambda_e)^4\,\omega_e^2 + \gamma^2 \gg \left(\omega_o - 3\,\frac{k_o}{k}\,(k\lambda_e)^2\,\omega_e\right)^2 \quad . \tag{8}$$

We note here that in the opposite limit (i.e., $k \ll k_o$) the parametric decay instability is obtained. However, the threshold condition for the decay instability,

$$\frac{W_o}{n_o T_e} > \tfrac{1}{8}\,\frac{m}{M} > 6(k_o\lambda_e)^2 \ ,$$

is typically higher than that for the OTS instability, and we confine the discussion in this paper to the OTS instability. In addition, we observe that the predominant direction of energy transfer by this process is toward $k > k_o$ (i.e., toward shorter wavelengths).

The effect of small, but finite, bandwidths can also be included analytically when, in addition to (8), we have

$$\gamma \gg 3\,\frac{\Delta k_o}{k}\,(k\lambda_e)^2\,\omega_e \ . \tag{9}$$

In this case the threshold condition is of the form

$$\frac{W_o}{n_o T_e} > 3(k\lambda_e)^2 \left[1 - 4\,\frac{k_o^2}{k^2} + 4\,\frac{\Delta k_o^2}{k^2}\right] \ , \tag{10}$$

and we have that ω_o is given approximately by (14) and

$$\gamma^2 \cong \tfrac{3}{4}\,\omega_e^{\,2}\,\frac{\pi}{M}\,(k\lambda_e)^2\left[\frac{W_o}{n_o T_e} - 3(k\lambda_e)^2\left(1 - 4\,\frac{k_o^{\,2}}{k^2} + 4\,\frac{\Delta k_o^{\,2}}{k^2}\right)\right]$$

$$\times\left[\frac{m}{M} + \tfrac{9}{4}\,(k\lambda_e)^2\left(1 - 4\,\frac{k_o^{\,2}}{k^2} + 4\,\frac{\Delta k_o^{\,2}}{k^2}\right)\right]^{-1} \qquad (11)$$

It is clear that, in contrast to the effect of finite k_o, the effect of finite Δk_o is to increase the instability threshold.

The scaling of the OTS growth rate with the spectral energy density of the beam-driven modes can be obtained from either (7) or (11) in the dipole approximation (i.e., $k_o = \Delta k_o = 0$). In the regime in which $3(k\lambda_e)^2 < W_o/n_o T_e < m/M$, the maximum growth rate is given by

$$(\gamma/\omega_e)_{max} \cong \tfrac{1}{4}\,\frac{W_o}{n_o T_e} \quad . \qquad (12)$$

On the other hand, when $W_o/n_o T_e > 3(k\lambda_e)^2, m/M$ we find

$$(\gamma/\omega_e)_{max} \cong \left(\tfrac{1}{3}\,\frac{m}{M}\,\frac{W_o}{n_o T_e}\right)^{\frac{1}{2}} \qquad (13)$$

The complete dispersion relation has also been studied numerically, for cases in which k and k_o are comparable, to determine the scaling of γ with k_o when $k_o/k \sim 1$. The results are shown in Fig. 9 in which we plot the maximum growth rate as a function of $k_o\lambda_e$ for various choices of $W_o/n_o T_e$. We note here that peak growth has been found to occur for $k \leq 2k_o$ in the cases considered. As seen in the figure, this scaling is

dependent upon W_o/n_oT_e, but γ_{max} is relatively independent of k_o for $k_o\lambda_e \lesssim .02$. However, for higher values of $k_o\lambda_e$ $(0.02 < k_o\lambda_e < 0.10)$ the scaling ranges between $\gamma_{max} \sim (k_o\lambda_e)^{.18} - (k_o\lambda_e)^{.49}$, depending upon W_o. It should also be pointed out that the transition region for $k_o\lambda_e \simeq .02$ corresponds to those modes with group velocities comparable to the ion sound speed.

Solution of the dispersion equation in the case in which ν_{ik}, ν_{ek}, and γ_k are nonzero yields little additional insight in relation to the complexity of the problem, and we limit ourselves here to a discussion of the necessary threshold condition in the dipole approximation. The approximate threshold condition,

$$\frac{W_o}{n_oT_e} > 3(k\lambda_e)^2 \left[1 - 4\frac{k_o^2}{k^2} + \frac{4}{9}(k\lambda_e)^{-4}\frac{\Gamma^2}{\omega_e^2}\right] , \qquad (14)$$

is obtained by setting $\omega = 0$. It is clear that, as in the case of finite Δk_o, the effect of damping is to enhance the instability threshhold, thereby, causing the transfer of energy by this mechanism to be less favorable and raising the saturation level of the beam-driven modes. We note, also, that in the dipole limit, the resulting dispersion equation is similar, but not identical, to the one considered by Nishikawa. The difference arises from the fact that the coupling coefficient between the ion and Langmuir modes (λ in Nishikawa's notation [11]), and which is the

coefficient of the nonlinear term in (2), was assumed by Nishikawa to be constant. Here, the coupling coefficient is k-dependent and depends on the frequency mismatch between the pump spectrum and the excited Langmuir waves (i.e., $\frac{\omega}{2} k^2 \lambda^2_e \omega_e$).

B. The Phenomenological Description

The phenomenological model is based upon the linearized theory of the parametric interactions. We consider the wave spectrum to be composed of two groups of high frequency Langmuir waves, one of which is resonant with the beam and is denoted by W_o and one composed of the nonresonant waves denoted by W_1, and the ion waves designated by W_s. There are two regimes of interest in this work: the initial stabilization of the linear instability (i.e., the sudden onset of the turbulence process), and the subsequently established asymptotic, quasi-steady state. The energy balance between these groups of spectrum is provided by both linear and nonlinear mechanisms. In the case of the beam-resonant waves, W_o, the principal source of energy is the linear beam-plasma instability, and energy is lost through the parametric coupling with other modes. The nonresonant spectra (i.e., W_1 and W_s) can grow only by means of the nonlinear transfer mechanism, and are subject to damping by the background plasma. We note here that linear damping of the beam-resonant spectrum is excluded due to the high phase velocities of the waves involved.

The time evolution of the system in the initial stabilization-phase can be described by the following set of rate equations

$$\frac{\partial}{\partial t} W_o = 2\gamma_o W_o - 2\gamma(W_o)\, W_1 \,, \qquad (15)$$

$$\frac{\partial}{\partial t} W_1 = 2\gamma(W_o) W_1 , \tag{16}$$

where γ_o is the linear growth rate of the electron beam instability, and $\gamma(W_o)$ is the nonlinear transfer rate which is equivalent to the growth of the oscillating two stream or parametric decay instabilities. For simplicity, we consider only the transfer of energy between the pump and the fastest growing mode in the dipole approximation.

In the limit in which $3(k\lambda_e)^2 < W_o/n_oT_e < m/M$, we have that

$$\frac{\partial}{\partial \tau} \frac{W_o}{n_oT_e} = 2\gamma_o - \tfrac{1}{2}\omega_e \frac{W_1}{n_oT_e} \tag{17}$$

$$\frac{\partial}{\partial \tau} \frac{W_1}{n_oT_e} = \tfrac{1}{2}\omega_e \frac{W_1}{n_oT_e} \tag{18}$$

where

$$\tau = \int_o^t dt' \frac{W_o}{n_oT_e} \tag{19}$$

Equations (17) and (18) may be solved immediately to obtain

$$\frac{W_o}{n_oT_e} = \left(\frac{W_o}{n_oT_e}\right)_{initial} + 2\gamma_o\tau - \left(\frac{W_1}{n_oT_e}\right)_{initial}[\exp(\omega_e\tau/2) - 1] , \tag{20}$$

$$\frac{W_1}{n_oT_e} = \left(\frac{W_1}{n_oT_e}\right)_{initial} \exp(\omega_e\tau/2). \tag{21}$$

On the basis of this set of equations, we can sketch the approximate behavior of the beam plasma system as a function of τ. Evidently, W_o increases linearly with τ (which corresponds to an exponential dependence on t) until the contribution of the second term on the right hand side of (17) becomes significant. The maximum value of the spectral energy density of the beam-driven modes occurs when $\tau = \tau_{max}$, where

$$\tfrac{1}{2}\,\omega_e \tau_{max} = \ell n \left[4\,\frac{\gamma_o}{\omega_e} \left(\frac{W_1}{n_o T_e} \right)^{-1}_{initial} \right] \tag{22}$$

Substitution of (22) into (20) yields

$$\left(\frac{W_o}{n_o T_e} \right)_{max} = \left(\frac{W_o}{n_o T_e} \right)_{initial} + 4\,\frac{\gamma_o}{\omega_e}\; \ell n \left[4\,\frac{\gamma_o}{\omega_e} \left(\frac{W_1}{n_o T_e} \right)^{-1}_{initial} \right] \tag{23}$$

Since the logarithmic variation in (23) provides only a weak variation with γ_o and $(W_1)_{initial}$, we have that $(W_o)_{max} \sim \gamma_o$ in this parametric regime.

In an analogous manner, it may be shown that in the regime in which $m/M,\ (k\lambda_e)^2 < W_o/n_e T_e$ the peak value of the spectral energy of the beam-driven modes is given approximately by

$$\left(\frac{W_o}{n_o T_e} \right)_{max} \simeq \tfrac{3}{4}\,\frac{\gamma_o^2}{\omega_e^2}\,\frac{M}{m} \left(\ell n \left[\left(3\,\frac{M}{m} \right)^{\frac{1}{2}}\,\frac{\gamma_o^2}{\omega_e^2} \left(\frac{W_1}{n_o T_e} \right)^{-1}_{initial} \right] \right)^2 . \tag{24}$$

As a result, the scaling is given by $W_o \propto \gamma_o^2$ in this regime. To summarize these results, we have that

$$\left(\frac{W_o}{n_o T_e}\right)_{max} \propto \begin{cases} \gamma_o \quad , \ \frac{3}{4}(k\lambda_e)^2 < \gamma_o/\omega_e < \frac{1}{4}\frac{m}{M} \\ \gamma_o^2 \quad , \ \frac{\gamma_o}{\omega_e} > 3^{-\frac{1}{2}}\frac{m}{M} \ , \ \left(\frac{m}{M}\right)^{\frac{1}{2}} \ (k\lambda_e) \end{cases} \tag{25}$$

within the context of the dipole approximation in which electron and ion damping are not included. Of course, it should be noted that since the inclusion of phenomenological damping results in a decrease in the growth rate of the oscillating two stream instability, the maximum value of the spectral energy density of the beam driven modes (as well as the level reached at saturation) will be higher than that predicted within the context of the dipole approximation.

Comparison of (25) with Fig. 4 shows that good agreement with the simulation can be achieved by such a phenomenological model, and we observe that not only are these two regimes in the scaling of $(W_o)_{max}$ and γ_o found, but the transition point is also in correspondence with the results of the simulation.

The scaling between $(W_o/n_o T_e)_{max}$ and $k_o\lambda_e$ can now be readily explained. The initial saturation occurs when the linear (γ_o) and nonlinear (γ_{NL}) energy transfer rates are in balance (i.e., $\gamma_o \lesssim \gamma_{NL}$). Therefore, if we consider the scaling of the mode with the fastest nonlinear growth for which (see Fig. 9) $\gamma_{NL} \simeq (k_o\lambda_e)^{.4}\ (W_o/n_o T_e)^{\frac{1}{2}}$, then it is clear that stabilization will occur for

$$\left(\frac{W_o}{n_o T_e}\right)_{max} \simeq \gamma_o^2\ (k_o\lambda_e)^{-.8} \ ,$$

which is in qualitative agreement with the results of the simulation.

The asymptotic state is, perhaps, the least explored regime in the study of this nonlinear stabilization mechanism; however, guided by the simulation results, we will discuss a phenomenological approach in this regime as well. In the strongly turbulent regime we must also include the low frequency fluctuations in the analysis. We define $W_s = \sum_k (\delta n_k/n_o)^2$, and attempt to fit the simulation results to the following set of equations, for $T_e \approx T_i$,

$$\frac{\partial}{\partial t}\frac{W_o}{n_o T_e} = 2\gamma_o \frac{W_o}{n_o T_e} - \nu^* \frac{W_o}{n_o T_e} \quad , \tag{26}$$

$$\frac{\partial}{\partial t}\frac{W_1}{n_o T_e} = \nu^* \frac{W_o}{n_o T_e} - \nu_1 \frac{W_1}{n_o T_e} \, , \tag{27}$$

and

$$\frac{W_1}{n_o T_e} = 2\, W_s^{\frac{1}{2}} \quad . \tag{28}$$

These equations reflect the difference between the quasi-steady asymptotic regime and the linear phase of the interaction; specifically, the presence of finite amplitude ion acoustic waves and cavities allows a mechanism for the dissipation of long wavelength Langmuir waves via scattering off density fluctuations (i.e., the Dawson-Oberman high frequency resistivity[12]). This process is included in the term $\nu^* W_o$, where

$$\nu^* = \beta (k\lambda_e)^{-2} W_s \omega_e \tag{29}$$

and β is a factor which depends upon the detailed character of the spectra. Under the assumption that the density and electric field perturbations satisfy the pressure balance condition, we expect $W_s^{\frac{1}{2}} \simeq 6(k\lambda_e)^2$ from which it follows that $\nu^* \simeq 6\beta\, W_s^{\frac{1}{2}}\omega_e$. Equation (28) follows from pressure balance considerations. The damping of the W_1 spectrum is modelled by the term in ν_1.

A basic aim in this paper is to determine how well the phenomenological description of Eqs. (28)-(30) approximates the simulation results for the stationary state. Under the assumption of a steady state, Eq. (28) implies that

$$\gamma_o \simeq 3\beta W_s^{\frac{1}{2}}\omega_e. \tag{30}$$

As seen in Fig. 4, such an approximate relationship holds for the range of the simulations with $\beta \simeq .025$. Equation (27) yields $\nu^* W_o = \nu_1 W_1$ in the steady state regime; therefore, the energy deposition in the system ($2\gamma_o W_o$) will scale as $2\gamma_o W_o \simeq 27\, \nu_1 \gamma_o\, n_o T_e/\omega_e$. Comparison with Fig. 5 bears out this scaling for $\nu_1 \simeq 10^{-3}\omega_e$. This value of ν_1 corresponds to Landau damping for the mode corresponding to $k_1\lambda_e \simeq .21$ (or an equivalent phase velocity of about $5.1\, v_e$). An important conclusion to be drawn from this scaling is the linear relationship between the energy deposition rate and γ_o. Finally, Eq. (28) was compared with the simulation results and agreement was found to be better than 40%.

IV. Summary and Discussion

In the present work, we have subjected a theory of the stabilization of the resonant beam plasma instability by a nonlinear coupling of Langmuir and ion acoustic fluctuations to a detailed analytic and numerical study. The interaction proceeds via the oscillating two stream-instability which can be important if the spectral energy density of the beam-generated spectrum of Langmuir oscillations exceeds threshold. At this point, both shorter wavelength (with correspondingly lower phase velocities) Langmuir oscillations and ion acoustic fluctuations are driven unstable, and the transfer of energy from the spectrum of waves in resonance with the beam can become important. As a consequence, the peak value of the beam-driven waves (and, hence, stabilization of the interaction) occurs when the nonlinear transfer of energy to the non-resonant Langmuir modes and ion acoustic oscillations balances the linear growth of the resonant waves.

It should be noted that effects due to spontaneous emission, stimulated scattering, electromagnetic mode coupling, particle trapping and pitch angle diffusion have been neglected in the analysis. In addition, parametric decay interactions, which tend to transfer energy to longer wavelength modes with higher phase velocities, were neglected in the treatment. The importance of these effects, however, must be determined for specific applications of the theory.

The most important aspects of this work are the determination of scaling laws between the growth rate of the linear beam-plasma instability and the fluctuation levels in the electric field and plasma density attained at the initial stabilization and in the asymptotic state,

as well as the formulation of a phenomenological description of the process. Estimates of the scaling of the spectral energy density of the beam-resonant modes and the ion density fluctuations are obtained by consideration of the nonlinear transfer rates. To this end, we include a brief discussion of the effects of finite wavelength and finite wavelength spread in the pump spectrum on the growth rate of the OTS instability. A discussion of the effects of electron and ion damping on the growth rate is also included. On the basis of this study, estimates of the scaling of the spectral energy density of the beam-resonant spectrum at the point of initial stabilization are obtained. Specifically, it is found that the peak spectral energy density of the beam-driven modes is directly proportional to the linear growth rate for $\gamma_o/\omega_e \lesssim m/M$, and is proportional to the square of the linear growth rate otherwise. This is found to be in substantial agreement with the results of the numerical simulation. Agreement is also demonstrated for the predictions of the phenomenological model and the results of the simulation in the asymptotic regime. Quantitative estimates of the level at which peak spectral energy densities occur are found, however, to be sensitive to the levels of electron and ion damping included as well as to the central wavelength and wavelength spread of the pump spectrum. It was also demonstrated by the numerical simulation of Eqs. (1) and (2) that the parametric saturation mechanism is intimately associated with the process of soliton formation.

An immediate application of the parametric stabilization mechanism is to electron streams in the solar wind; specifically to the case of type III solar bursts. Here, the electron streams have been observed

to propagate large distances with small energy loss, which is in contrast to the predictions of the quasilinear theory. It has been shown, further, that for parameters typical to such streams the nonlinear stabilization mechanism described in this work is appropriate. Experimental verification of the action of this mechanism would be provided by the observation of solitons in conjunction with the electron streams. However, direct measurement of soliton fields in the solar wind is, at the present time, difficult and we must rely on indirect methods. In particular, electromagnetic radiation with $\omega \sim 2\omega_e$ has been observed to be associated with type III solar bursts. The intensity of this radiation is seen to scale linearly with the stream for weak electron fluxes, and to scale with the square of the stream density when the electron flux rises above a certain level. Since Langmuir solitons may be expected to emit $2\ \omega_e$ radiation and since the linear beam-plasma growth rate is directly proportional to the electron density, an estimate of the scaling of the radiation intensity with the linear growth rate can, in principle, be obtained which is based on the stabilization mechanism described here. It has been shown that the volume emissivity of $2\ \omega_e$ radiation from densely packed Langmuir solitons depends linearly on W_o. Consequently, the radiation intensity is expected to scale linly with the electron density for weak electron fluxes and quadratically for strong fluxes. As mentioned previously, this is in accord with observations.

Another important consequence of the present work is its application to plasma heating by means of relativistic electron beams. For long beam pulses, the energy deposition during the initial phase of the interaction is small (i.e., $W_o/n_o T_e < 1$) and it is suffiecient to consider the asymptotic regime. From Eqs. (26) - (28), it can be shown that the stopping length for a relativistic

beam with energy $\varepsilon_b = \delta mc^2$ per electron (where δ is the relativistic factor) is of the order of

$$L \approx .02 \frac{c}{\nu_1} \frac{(\delta - 1)mc^2}{T_e} (1 + \delta). \tag{31}$$

The important observation which arises from the above relation is the dependence of the stopping length on $(\nu_1 T_e)^{-1}$. As a consequence, since ν_1 describes absorption by the thermal plasma, it is clear that short coupling lengths will result from having beams interact with preheated plasmas. For example, if the end plugs of a tandem mirror were preheated to 10 keV, the stopping distance expected will be of the order of 5m for typical operating parameters (and $\nu_1 \approx .001\omega_e$). It should also be noted from the preceding equations that background plasma heating will be governed by

$$\frac{\partial T_e}{\partial t} \approx 54\nu_1 \frac{\gamma_o}{\omega_e} T_e, \tag{32}$$

which implies that the plasma temperature will increase exponentially. When $\nu_1/\omega_e \approx .001$, the exponentiation time is of the order of $20\gamma_o^{-1}$, which suggests that long pulses will play a more effective role in heating plasmas. These aspects, as well as detailed pulse shapes, will be discussed further in a future publication.

ACKNOWLEDGEMENTS

This work has been supported in part by the Office of Naval Research and in part by the National Aeronautics and Space Administration under contract W-14365.

Appendix: The Linearized OTS Dispersion Equation

Substitution of the Lorentzian spectrum (4) into the dispersion equation (3) yields an integrand with four poles in the complex k' plane which are located at

$$k' = k_o \pm i\Delta k_o,\ \frac{1}{2} k \left[\pm 1 + \frac{2}{3} \frac{(\omega + i\nu_{ek} - i\gamma_k)}{\omega_e (k\lambda_e)^2} \right].$$

When $k(\mathrm{Im}\ \omega + \nu_{ek} - \gamma_k) > 0$, there are three poles in the upper half-plane and one pole in the lower half-plane. Thus, if we integrate along the real k' axis and close the controur in the lower half-plane, then we pick up a single residue which corresponds to the pole at $k' = k_o - i\Delta k_o$. In the opposite case, we close the contour in the upper half-plane and the only contribution to the integral is due to the residue of the pole at $k' = k_o + i\Delta k_o$. The result is

$$\omega(\omega + i\nu_{ik}) - k^2 c_s^2 =$$

$$= -\frac{3}{4} \frac{m}{M} (k\lambda_e)^4 \frac{W_o}{n_o T_e} \frac{\omega_e^4}{\frac{9}{4}\omega_e^2 (k\lambda_e)^4 - \left[\omega + \Gamma - 3(k\lambda_e)(k_o\lambda_e)\omega_e\right]^2}, \tag{A-1}$$

where

$$\Gamma \approx \nu_{ek} - \gamma_k + 3\sigma_k |k| \Delta k_o \lambda^2{}_e, \tag{A-2}$$

and $\sigma_k = \mathrm{sgn}(\mathrm{Im}\ \omega + \nu_{ek} - \gamma_k)$. It is apparent that the effect of the finite bandwidth of the pump spectrum (i.e., Δk_o) appears as an effective damping mechanism; however, the appearance of the factor σ_k requires some physical interpretation. In the absence of the pump

spectrum the coupled ion and Langmuir waves are damped by the background plasma, and these waves can grow only at the expense of energy from the beam-driven modes. When $\sigma_k > 0$ the effect of the finite bandwidth is dissipative, and there is effective enhancement in the damping decrement of the coupled Langmuir waves. On the other hand, when $\sigma_k < 0$ there is an effective "negative dissipation" with respect to the pump waves. In both cases, the effect of nonzero Δk_o is to inhibit the transfer of energy to the coupled acoustic and Langmuir modes. As a consequence, the broadening of the pump spectrum is expected to result in an enhancement in the levels of the beam-driven waves when stabilization is achieved.

In general, Eqs. (A-1) and (A-2) represent a quarter dispersion equation with complex coefficients

$$\omega^4 + a_3\omega^3 + a_2\omega^2 + a_1\omega + a_o = 0,$$

where

$$a_3 \equiv -6(k\lambda_e)(k_o\lambda_e)\omega_e + i(2\Gamma + \nu_{ik}),$$

$$a_2 \equiv -\left[\Omega_k^2 + k^2c_s^2 + 2\nu_{ik}\Gamma + 6i(k\lambda_e)(k_o\lambda_e)\omega_e(\Gamma + \nu_{ik})\right],$$

$$a_1 \equiv 6(k\lambda_e)(k_o\lambda_e)\omega_e(k^2c_s^2 + \nu_{ik}\Gamma) - i(\nu_{ik}\Omega_k^2 + 2k^2c_s^2\Gamma)$$

$$a_o \equiv k^2c_s^2\Omega_k^2 - U_o^2\omega_e^4 + 6(k\lambda_e)(k_o\lambda_e)\omega_e\Gamma\, k^2c_s^2 ,$$

and

$$\Omega_k^2 \equiv \frac{9}{4} (k\lambda_e)^4 \omega_e^2 \left(1 - 4 \frac{k_o^2}{k^2}\right) + \Gamma^2 ,$$

$$U_o^2 \equiv \frac{3}{4} \frac{m}{M} (k\lambda_e)^4 \frac{W_o}{n_o T_e} .$$

References

1. A. Mohri, K. Narihara, T. Tsuzuki, Y. Kubota, K. Ikuta, and M. Masuzaki, Proceedings of the Seventh International Conference on Plasma Physics and Controlled Nuclear Fusion Research, International Atomic Energy Agency, Innsbruck, Austria, 1978, Report X-5.
2. K. Papadopoulos, B. Hui, N. Winsor, Nucl. Fusion 17, 1087 (1972).
3. K. Papadopoulos, Phys. Fluids 18, 1769 (1975).
4. B. N. Breizman and D. D. Ryutov, Nucl. Fusion 14, 873 (1974).
5. A. A. Galeev, R. Z. Sagdeev, V. D. Shapiro, V. I. Shevchenko, Zh. Eksp. Teor. Fiz. 72, 507 (1977) [Sov. Phys. - JETP 45, 266 (1977)].
6. V. N. Tsytovich, Physics 82C, 141 (1976).
7. D. A. Hammer, K. A. Gerber, W. F. Dove, G. C. Goldenbaum, B. G. Logan, K. Papadopoulos, and A. W. Ali, Phys. Fluids 21, 483 (1978).
8. R. A. Smith, M. L. Goldstein, and K. Papadopoulos, Solar Phys. 46, 515 (1976).
9. W. M. Manheimer and K. Papadopoulos, Phys. Fluids 18, 1391 (1975).
10. V. E. Zakharov, Zh. Eksp. Teor. Fiz. 62, 1745 (1972) [Sov. Phys. - JETP 35, 908 (1972)].
11. K. Nishikawa, J. Phys. Soc. Jap. 24, 916 (1968); J. Phys. Soc. Jap. 24, 1152 (1968).
12. J. Dawson and C. Oberman, Phys. Fluids 5, 517 (1962).
13. H. Rowland and K. Papadopoulos, Phys. Rev. Lett. 39, 1276 (1977); H. Rowland, Ph.D. Thesis, Univ. of Maryland (1977); H. Rowland, Phys. Fluids (submitted for publication).
14. K. Papadopoulos and H. P. Freund, Comments on Plasma Phys. and Controlled Fusion (to be published).
15. K. Papadopoulos and H. P. Freund, Geophys. Res. Lett. 5, 881 (1978).

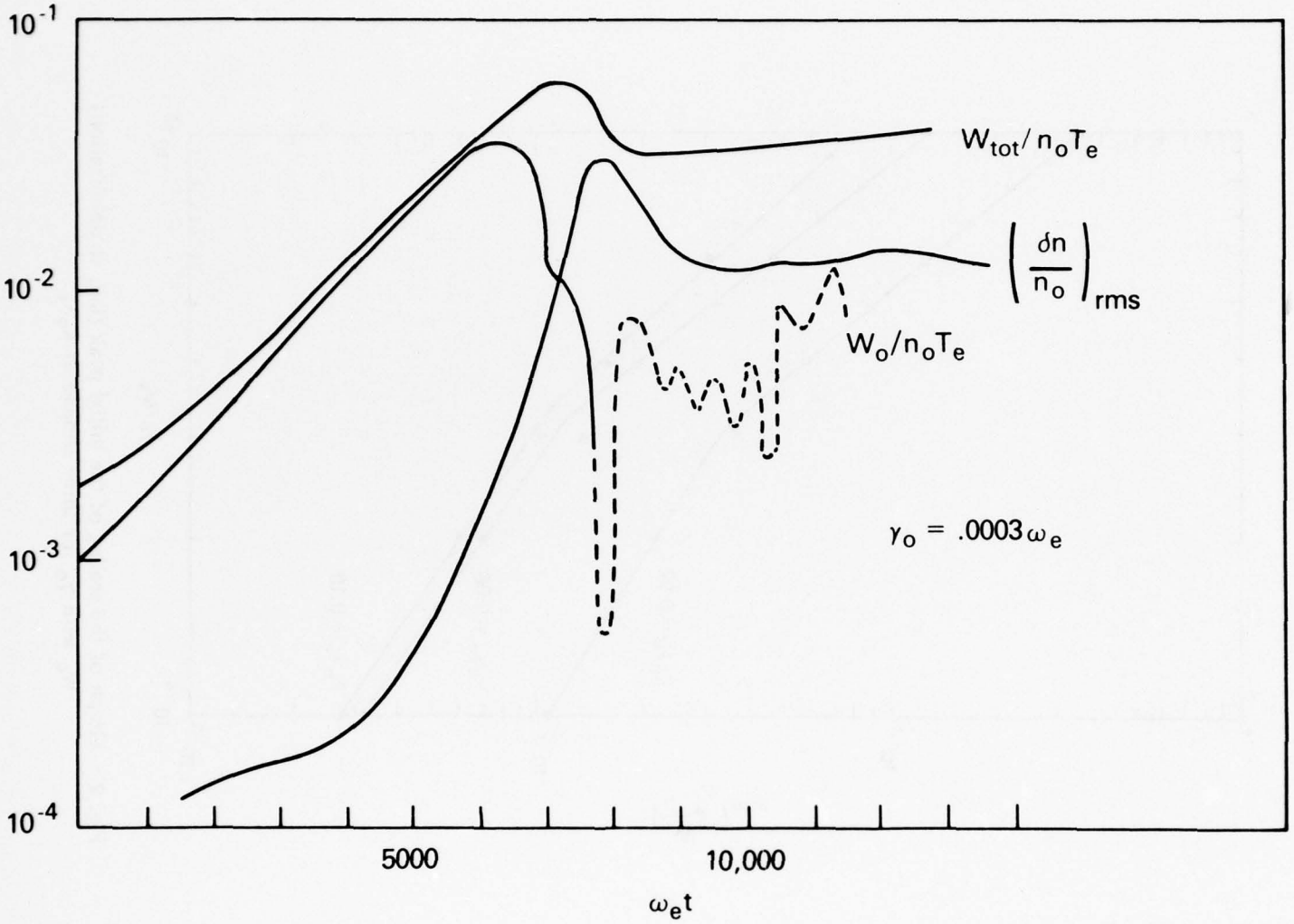

Fig. 1 — Graph of the time history of W_{tot}, W_o, and $(\delta n/n_o)_{rms}$

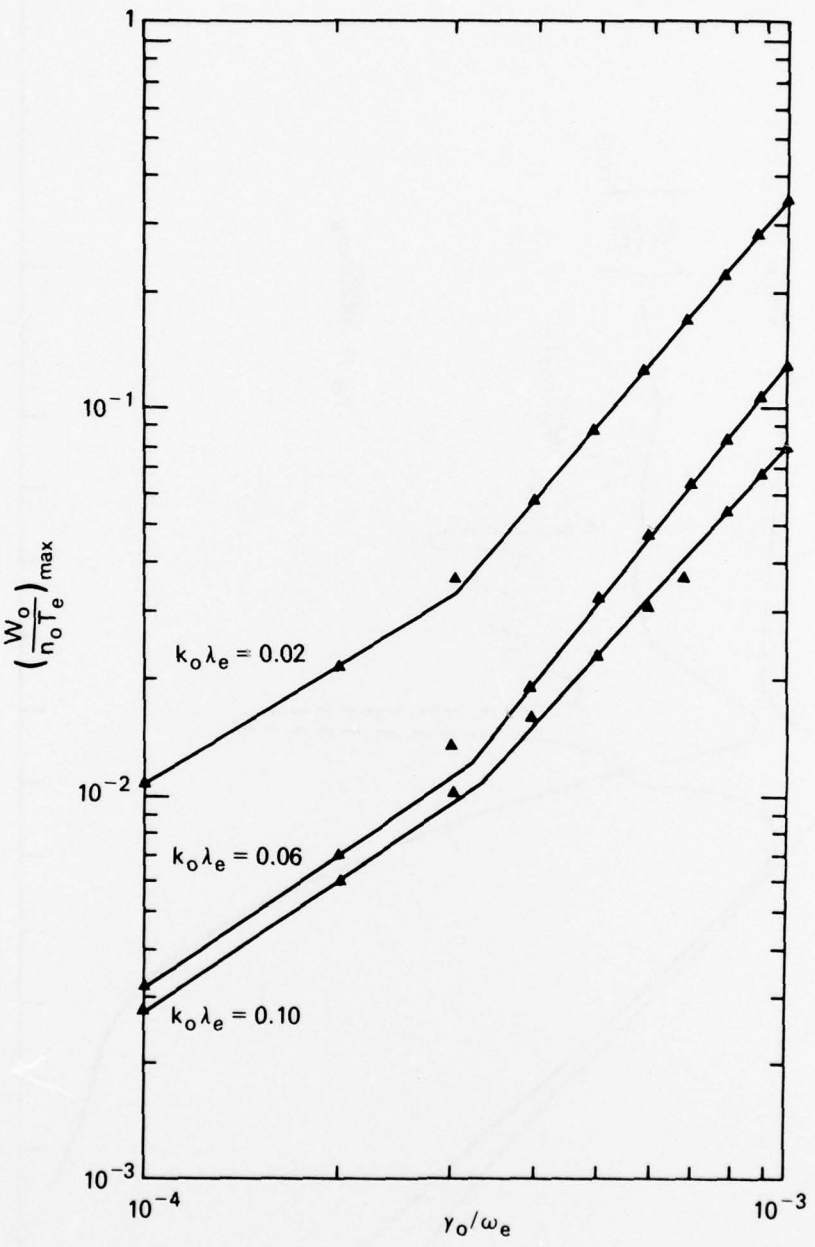

Fig. 2 — Graph of the scaling of the initial peak (i.e., at stabilization) W_o with γ_o for three choices of $k_o\lambda_e$

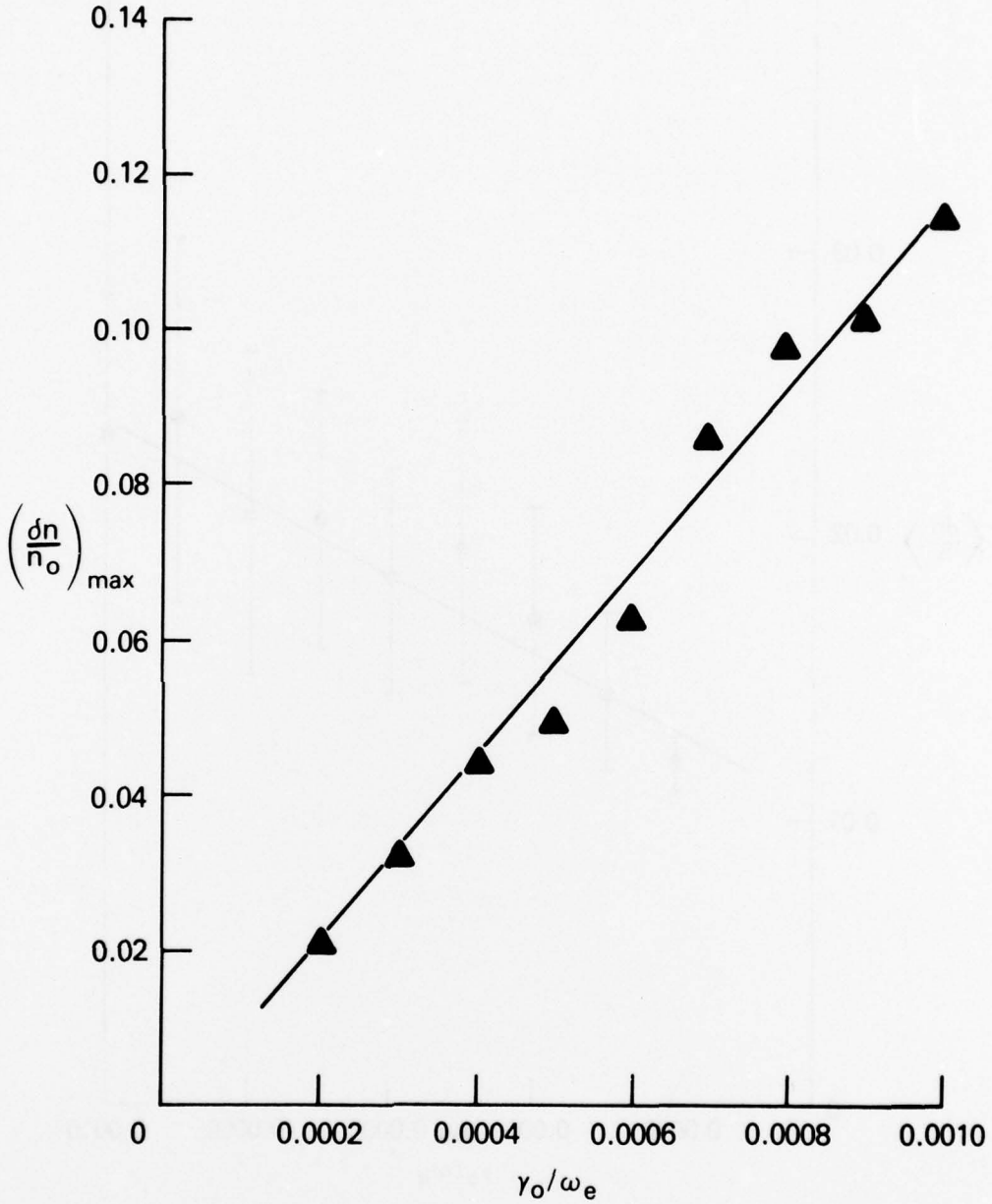

Fig. 3 — Graph showing the scaling of the value of $(\delta n/n_o)_{rms}$ versus γ_o at the initial stabilization

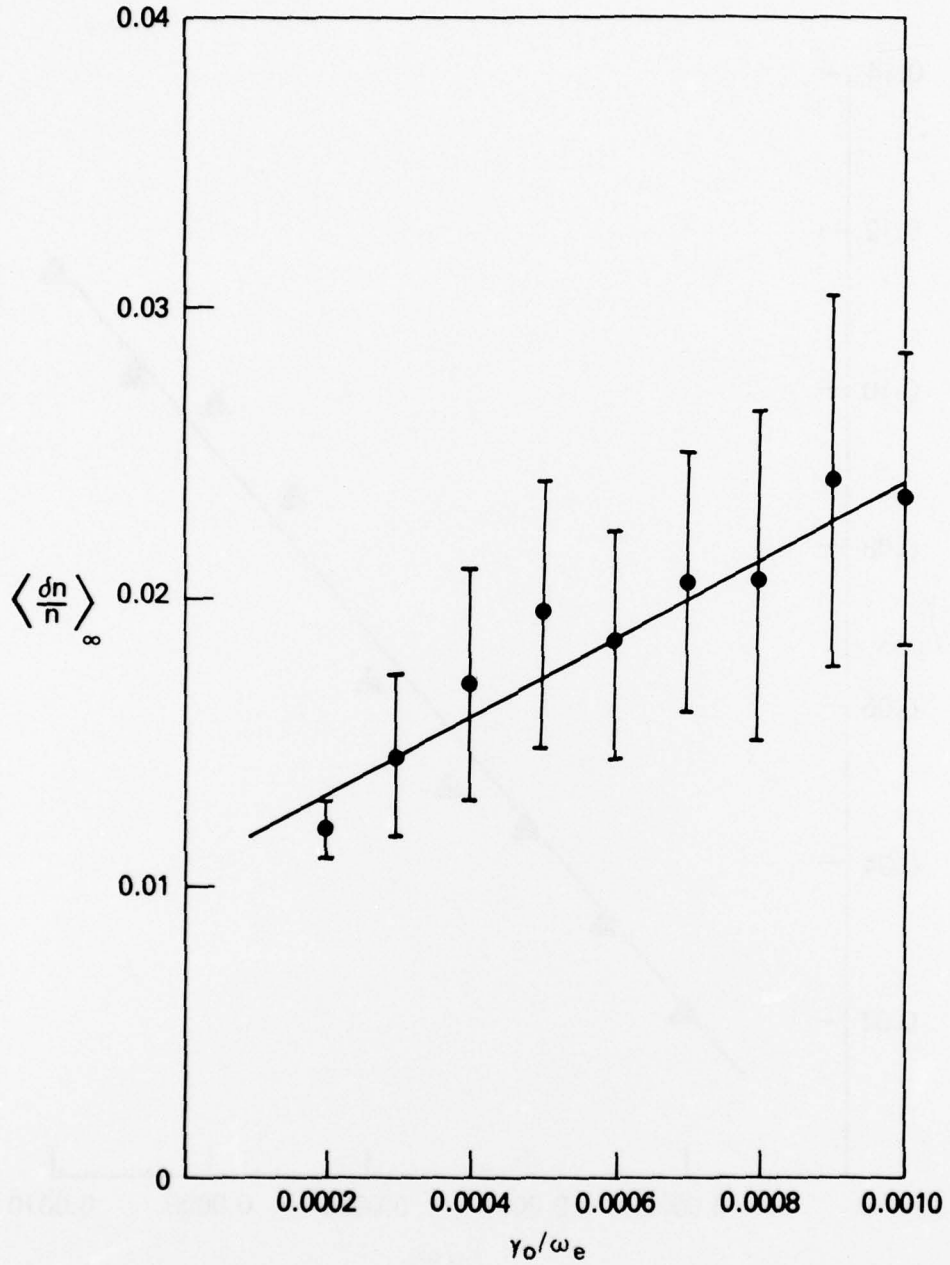

Fig. 4 — Plot of the average value of $(\delta n/n_o)_{rms}$ during the asymptotic state, versus γ_o

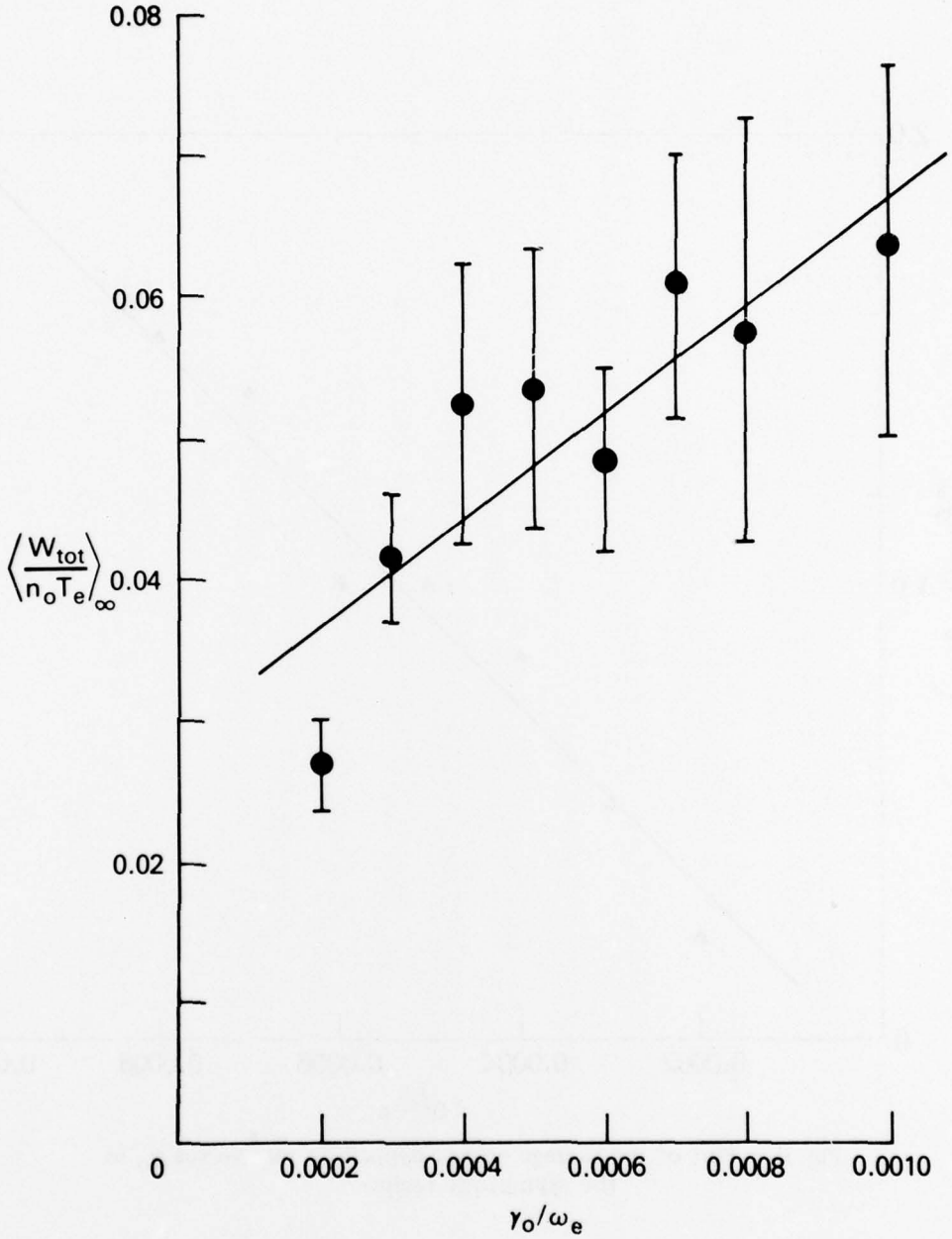

Fig. 5 — Plot of the average value of $W_{tot}/n_o T_e$, during the asymptotic state, versus γ_o

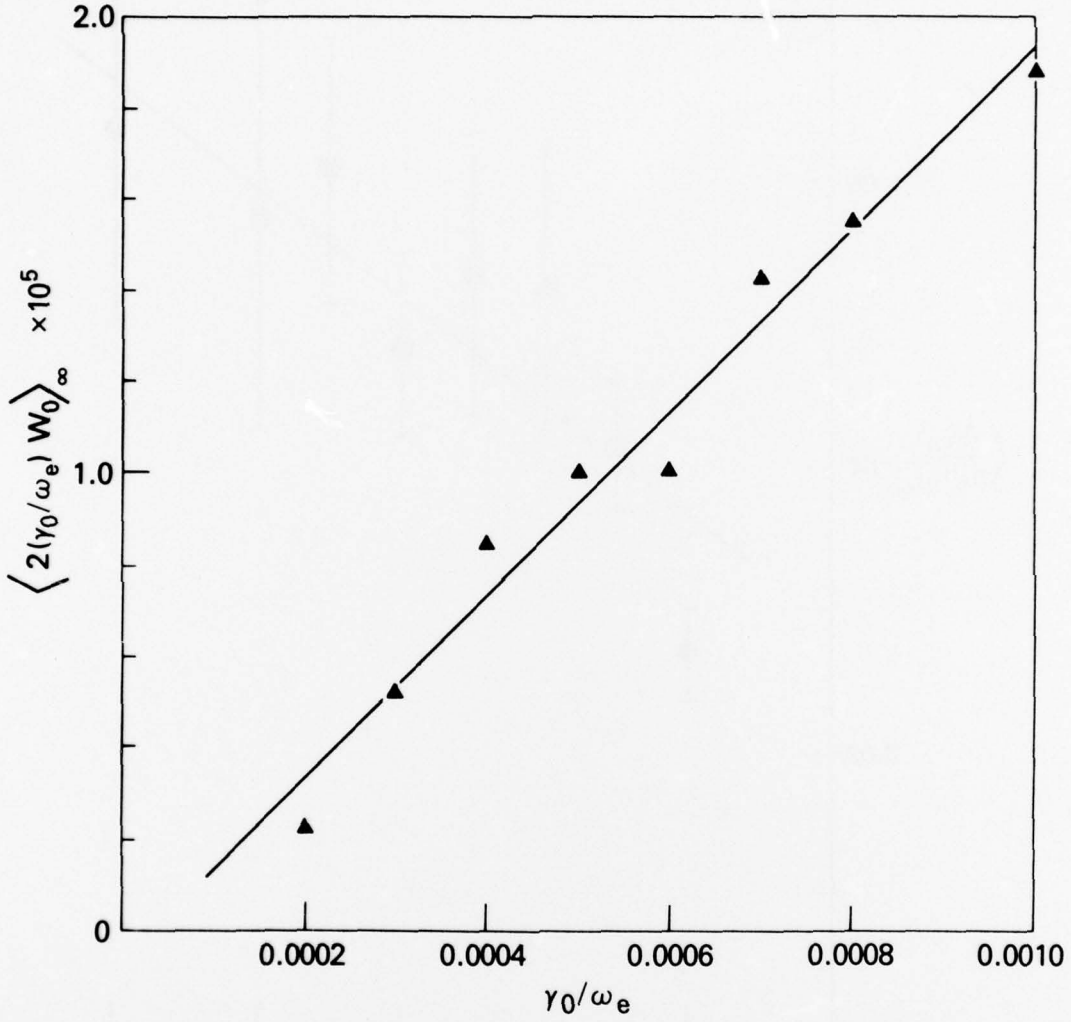

Fig. 6 — Plot of the average energy deposition rate versus γ_o in the asymptotic regime

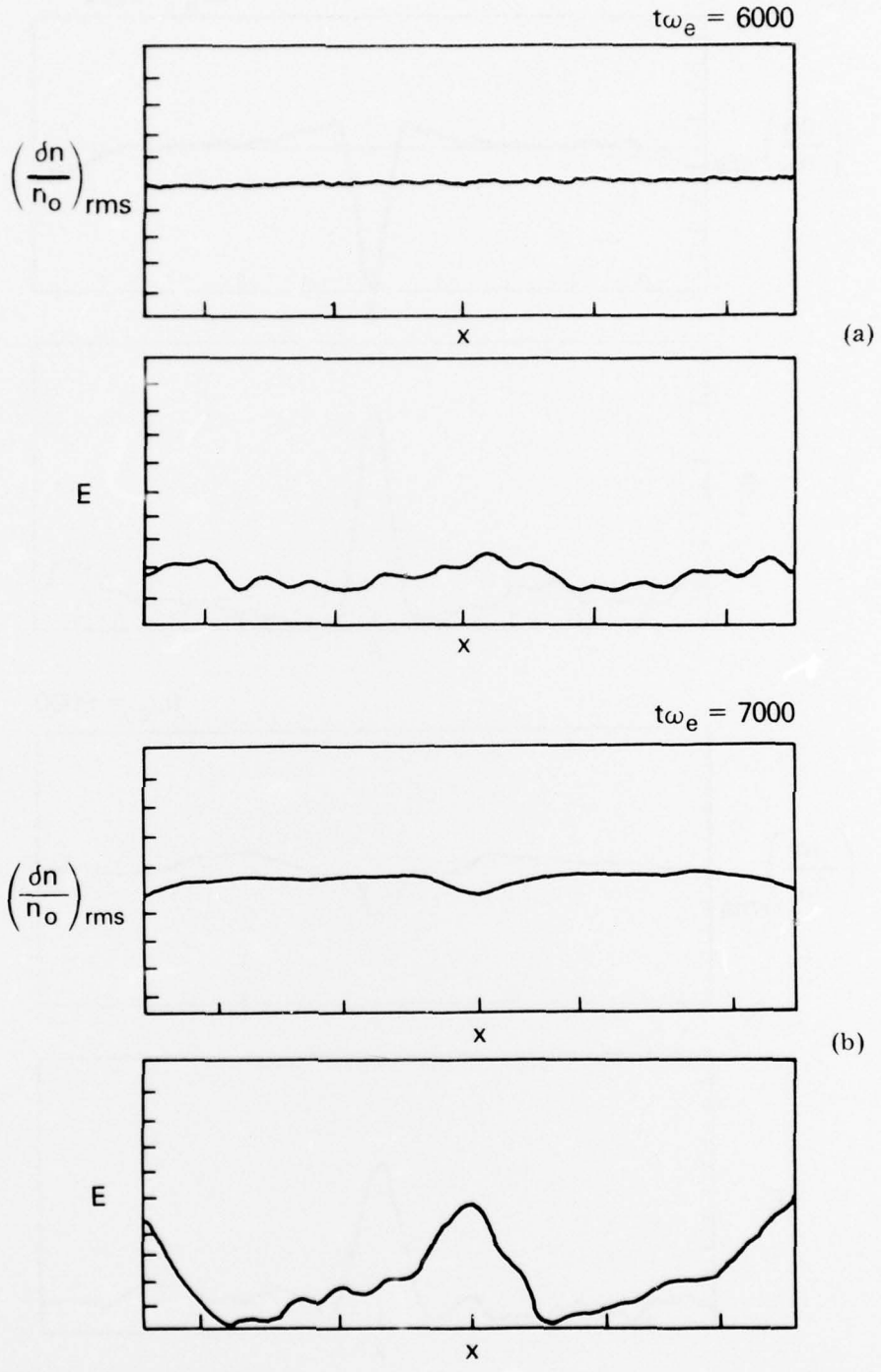

Fig. 7 — Graph showing the coordinate space representations of the electric field and plasma density fluctuations (a) in the linear phase of the interaction just prior to the onset of the turbulent phase, (b) when the peak in W_o is reached, (c) at the time of maximum amplitude of the spiky turbulence, and (d) during the asymptotic phase of the interaction.

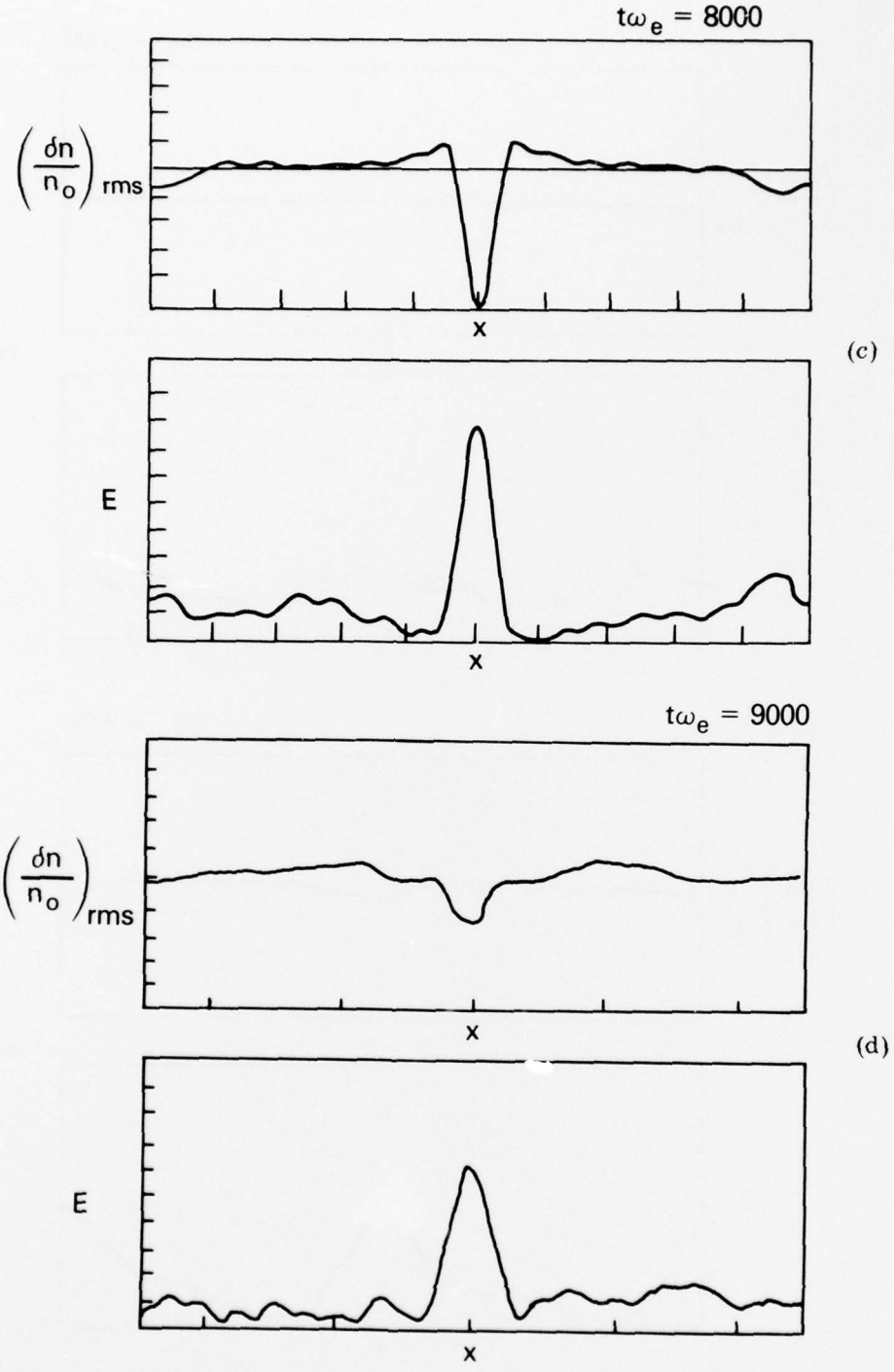

Fig. 7 — Graph showing the coordinate space representations of the electric field and plasma density fluctuations (a) in the linear phase of the interaction just prior to the onset of the turbulent phase, (b) when the peak in W_o is reached, (c) at the time of maximum amplitude of the spiky turbulence, and (d) during the asymptotic phase of the interaction.

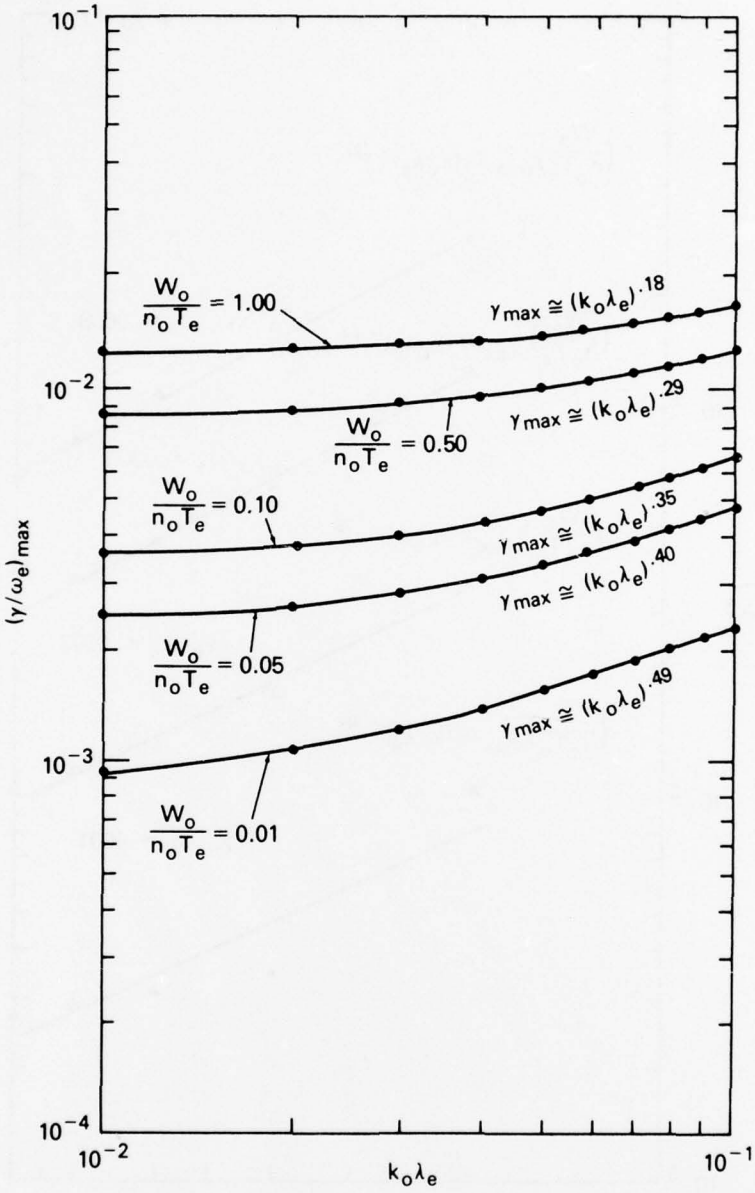

Fig. 8 — Graph of the scaling of the initial peak of W_o versus $k_o\lambda_e$ for several values of γ_o

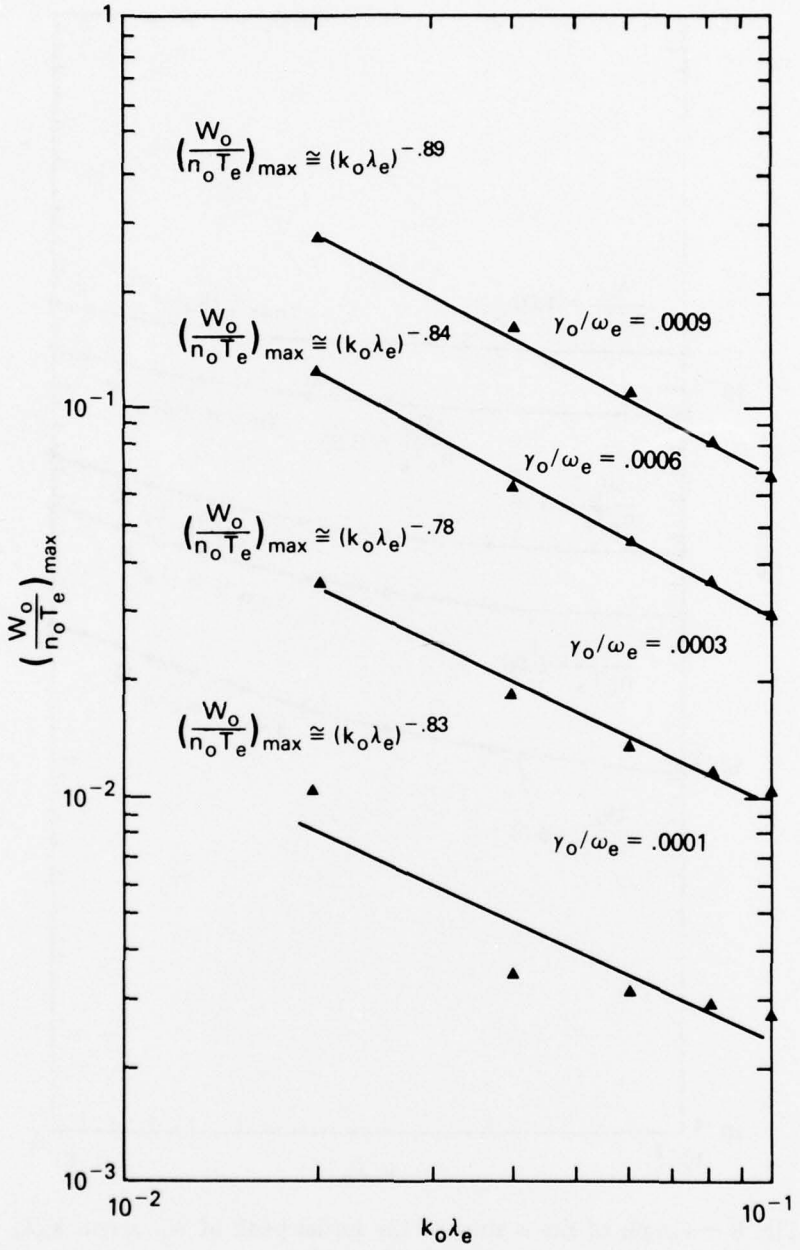

Fig. 9 — Plot of the maximum growth rate of the oscillating two stream instability versus $k_o\lambda_e$ for several choices of W_o/n_oT_e

DEPARTMENT OF THE NAVY

NAVAL RESEARCH LABORATORY
Washington, D.C. 20375

OFFICIAL BUSINESS
PENALTY FOR PRIVATE USE, $300

POSTAGE AND FEES PAID
DEPARTMENT OF THE NAVY
DoD-316
THIRD CLASS MAIL